Contribution of viscoelasticity in the dynamic simulation of HWD tests for flexible pavement assessment

R. Ktari[a,c], M. Broutin[b,*], B. Picoux[a], J. Neji[c], C. Petit[a]

[a] *Université de Limoges, Egletons, France*
[b] *STAC, Bonneuil-s-Marne, France*
[c] *LR-MOED-ENIT, Tunis, Tunisia*

Abstract

Modeling of a multilayered structure is presented in this paper. It allows simulating the dynamic behavior of flexible airfield pavement under the effect the loading applied by a nondestructive pavement assessment device: the Heavy Weight deflectometer (HWD). A Huet-Sayegh model is considered for the mechanical behavior of the bituminous layers. Benefits of viscoelastic behavior of bituminous materials are highlighted through this modeling.

Keywords: HWD ; dynamical backcalculation ; viscoelasticity.

Résumé

La modélisation d'une structure multicouche axisymétrique est présentée dans cet article. Elle permet la simulation du comportement dynamique d'une chaussée souple aéronautique sous l'effet d'un chargement avec un appareil d'auscultation non destructif : le Heavy Weight Deflectometer (HWD). Le comportement mécanique du revêtement est modélisé par un modèle viscoélastique qui correspond au modèle rhéologique Huet-Sayegh. Grâce à ce modèle dynamique l'apport du comportement viscoelastique des matériaux bitumineux est démontré.

Mots-clé: HWD ; calcul inverse dynamique ; viscoélasticité.

1. Introduction

The Heavy Weight Deflectometer (HWD) is a nondestructive pavement testing device. Its principle consists (Fig.1) in dropping a weight on the pavement through a load plate and buffer system, in order to generate an impulse transient stress simulating the load effect of an aircraft wheel pass. Surface deflections are recorded by 9 geophones laid on the pavement.

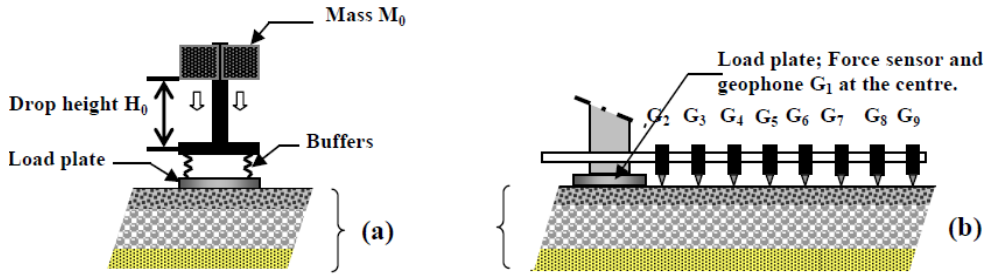

Fig.1. HWD measuring principle; (a) the falling weight; b) the geophones, from Broutin (2010)

Two dynamic time-domain models have been developed to study the dynamic behavior of a pavement structure and the characterization of its mechanical parameters:

- PREDIWARE by the French civil Aviation Technical Center (STAC) for the Heavy Weight deflectometer (HWD): Broutin (2010). This model allows automating backcalculation. It is based on the Cesar-LCPC finite element software (see Humbert et al. (2005)), and a regularized Gauss Newton algorithm. The structure is considered as linear elastic with global Rayleigh damping (limitation of current commercial CESAR version). It has been shown in Broutin (2010) that, on the one hand, the robustness of the iterative process of backcalculation is increased compared to conventional methods and, on the other hand, the backcalculated parameters are more realistic.
- PAVDYN by the Group for the study of heterogeneous Materials (GEMH) for the Falling Weight Deflectometer (FWD): El-Ayadi (2010). This model uses finite elements and is developed under Cast3M (Combescure, 2006). It is linear elastic with distinctive Rayleigh damping depending on the layer.

The identifications of the structural parameters of the pavement obtained using these two approaches (Broutin (2010) and El-Ayadi (2010)) appear to be much more accurate than those from conventional methods. They take into account the dynamic nature of the load and also the damping phenomenon occurring in pavement materials, which are not considered in the pseudo-static method. It appears that, whatever the model used, the Young's modulus of asphalt layers are generally underestimated. This result may come from the viscoelastic behavior of bituminous materials.

Many studies on semi-analytical viscoelastic modeling are presented in the literature (Chatti (1995), Chen (2011) or Duhamel et al. (2005)). The solution of the program using the spectral element DYNAPAV-UL (FWD) presented in Grenier (2009) is obtained by modeling in the frequency domain and considering horizontal wave-numbers. The mechanical behavior of asphalt layers is represented by a linear viscoelastic behavior with a hysteretic or a frequency dependent viscous damping.

It is used in Chupin, Chabot and Duhamel (2010) a semi-analytical method implying a model which takes into account the viscoelastic behavior of asphalt using the Huet-Sayegh model. This model is the base of the VISCOROUTE software.

In this paper, the effect of the contribution of viscoelastic behavior of these materials is presented through the dynamic response of the pavement structure. This study is based on a simplified version (three parameters instead of five) of the Huet's model presented in Huet (1963).

To consolidate the study, HWD tests were conducted in November 2011 on the STAC's test facility in Bonneuil-sur-Marne (France) presented in Broutin et al. (2008). Results from laboratory tests performed on the materials of this pavement are available to validate backcalculated moduli and damping ratios. As for the asphalt materials, complex moduli tests were performed by the Laboratoire Central des Ponts et Chaussées (LCPC).

2. Dynamical modeling

All materials are considered to exhibit isotropic linear elastic behavior. The system evolution is led by the usual dynamic equations:

$$\overrightarrow{div\underline{\underline{\sigma}}} + \vec{f} = \rho\vec{\gamma} \qquad in\ \Omega \tag{1}$$

The finite element discretization of the problem described by equation (1) leads to the classical expression:

$$[M]\ \ddot{u}(t) + [C]\dot{u}(t) + [K]\,u(t) = F(t) \tag{2}$$

where [M], [C] and [K] are respectively the mass, damping and stiffness matrices, u(t) the displacement vector and F(t) the external force vector.

A time-domain modeling has been developed for HWD data analysis. The model considers the applied dynamical load. This model is implemented in the finite element software Cast3M. It is based on 2D axis-symmetric layered mesh based on quadratic elements. Eight-node 2D elements have been used. A typical mesh for a standard flexible airfield pavement is presented in Fig. 2. It includes the load plate. Mechanical parameters of this model are given in Table 1.

The pavement structure is consists of four layers: 14.6 cm of Asphalt Concrete (AC_1), 17.8 cm of base Asphalt Concrete (AC_2), 54 cm of humidified Untreated Graded Aggregate (UGA) laid in two layers of 27 cm, and finally a layer of Subgrade (S) of about 5.2 m.

Boundary conditions are depicted in Fig. 2. The radial displacement is null on the axis due to symmetry considerations and the external boundary (U_R=0), as well as the vertical one at the bottom of the mesh (U_Z=0).

The model allows considering both fully bonded and fully frictionless interfaces.

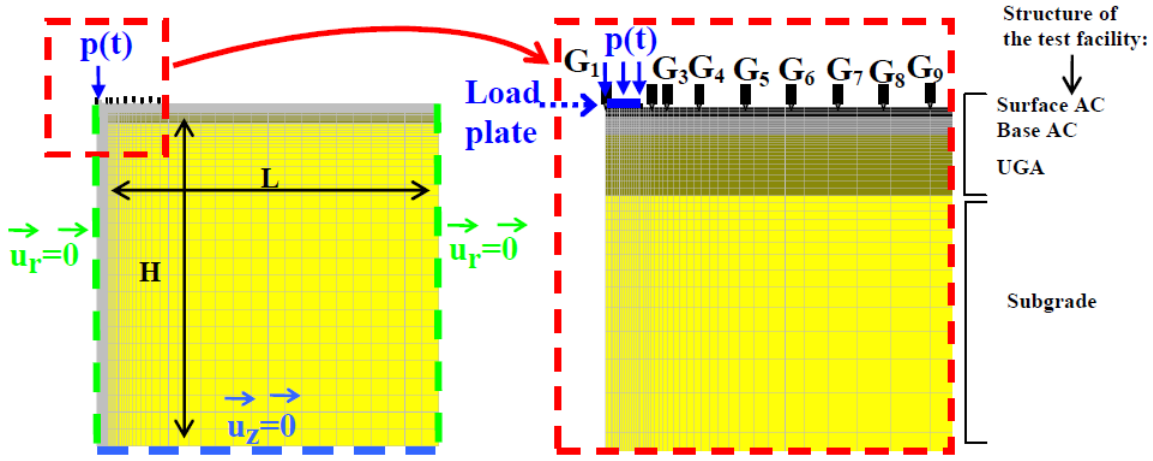

Fig.2.the mesh of the structure, from Broutin (2010)

Table 1. mechanical parameters

Layer	Material	Poisson's ratio	density [kg.m^{-3}]
0	load plate	0.25	6700
1	AC_1	0.3	2300
2	AC_2	0.3	2300
3	UGA	0.35	2100
4	UGA	0.35	2100
5	Subgrade	0.35	1800

The external action is here the actual recorded stress applied at each time step on the load plate during the HWD test. Pressure P(t) applied on the loading plate is considered as uniform. The HWD loading is measured (see Fig. 3) during the test by a force sensor integrated in the plate. The radius of the load plate is 0.225 m and the maximum of the force is 282.5 kN (1776.2 kPa). Respective radial distances of geophones from G_1 to G_9 is 0, 30, 40, 60, 90, 120, 150, 180 and 210 cm to the plate centre.

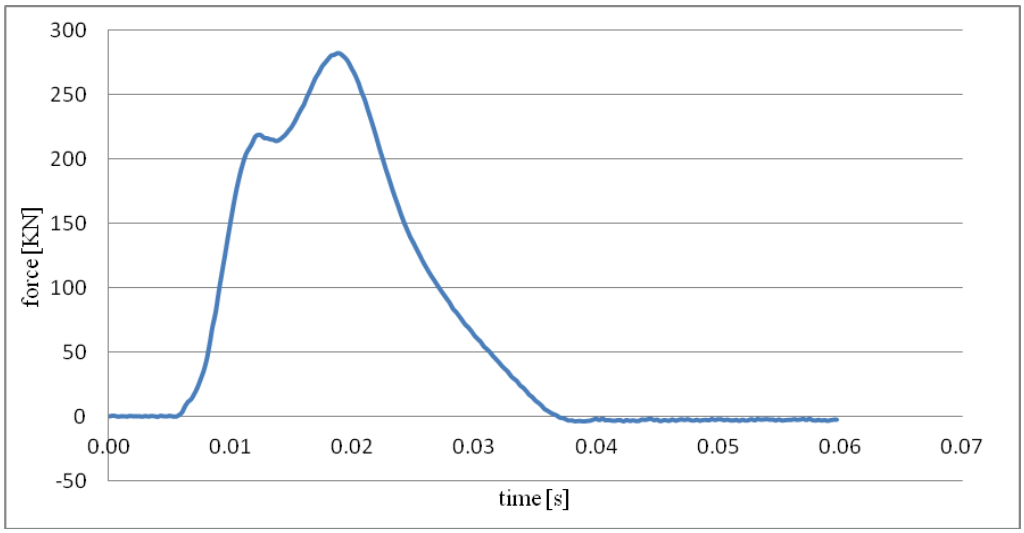

Fig.3. time-related applied force of HWD test

3. Preliminary results without damping

Using the model initially developed without damping (matrix [C] null), moduli of the different layers are adjusted until the numerical deflection basin matches with the experimental basin (Fig. 4). The farthest geophones allow determining the characteristics of the subgrade whereas the characteristics of the surface materials are obtained through geophones closest to the load center. This principle is used for the backcalculations with PAVDYN.

Although the model developed allows calibrating the experimental data by dynamic backcalculation on time histories (20 iterations), the results obtained with the PREDIWARE software in Broutin (2010) without damping show that they provide moduli values clearly underestimated compared to those expected on this kind of structure.

The norms of complex moduli obtained from laboratory tests on the Asphalted concrete AC_1 and AC_2 were used to check the consistency of the results with those corresponding to the pseudo frequency $f = 1/\Delta t = 33$Hz and at 18°C of the HWD test.

Table 2. comparison between numerical results Cast3M, PREDIWARE and experimental results of complex modulus

	AC1	AC2	UGA	UGA	Subgrade
Numerical Modulus (Cast3M) [MPa]	11300	14500	730	490	205
Modulus PREDIWARE [MPa]	2471	9337	704	560	66
Complex modulus (LCPC data) [MPa]	11155	16875			

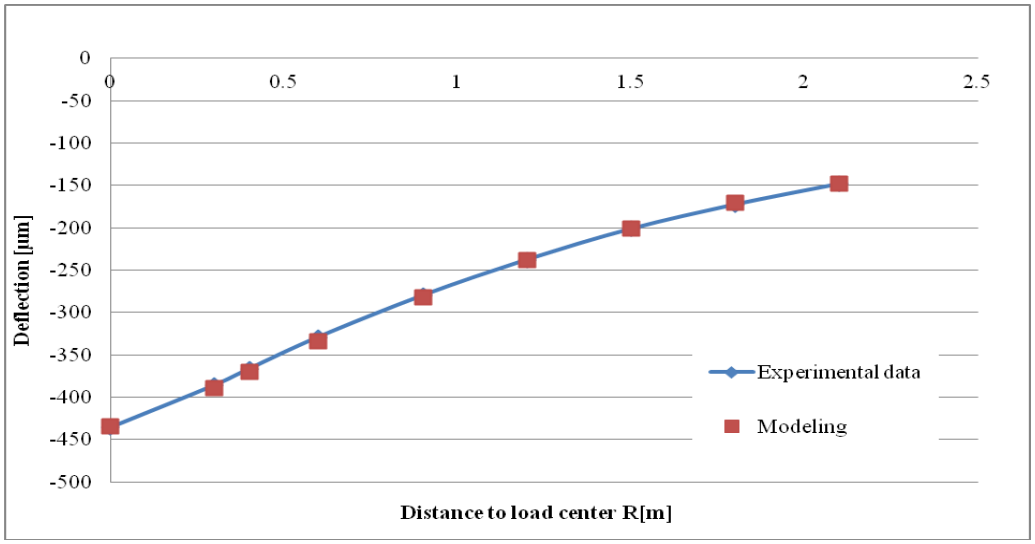

Fig.4. comparison between experimental and numerical values (elastic without damping)

4. Classical Rayleigh damping

4.1. Damping parameters

Only global Rayleigh damping is available so far in the CESAR-LCPC software. [C] is related to [M] et [K] thanks to the (3) relationship:

$$C = \alpha K + \beta M \qquad (3)$$

with α et β scalars, constant for the whole structure. These parameters are called Rayleigh coefficients. They are linked for each ω_i pulsation to the ξ_i damping ratio by the relation:

$$\xi i = \frac{1}{2}\left(\frac{\alpha}{\omega_i} + \beta\omega_i\right) \qquad (4)$$

The method consists in determining the α and β values to obtain damping as close as possible to $\xi_{moyenne}$ on a given range $[\omega_1, \omega_2] = 2\pi \times [frés; 60Hz]$. The drawback is the necessity to introduce a single value of global Rayleigh damping for the whole structure and not by layer. Cast3M gives the possibility of introducing a Rayleigh damping for each layer. The values used can be selected from the results of laboratory tests. Low frequencies may nevertheless be strongly damped. In practice, it is necessary that the damping remains constant over the frequency range of interest. The reduced damping is thus deduced from coefficients for the first ω_1 and second ω_2 natural frequencies and damping ratios ξ_1 and ξ_2 over the first and second natural frequencies of structure without damping. Assuming that the daming is the same for both frequencies ($\xi_1 = \xi_2 = \xi$), it comes:

$$\alpha = \frac{2\xi\omega_1\omega_2}{\omega_1+\omega_2} \quad \text{and} \quad \beta = \frac{2\xi}{\omega_1+\omega_2} \qquad (5)$$

For bituminous materials, ξ is determined experimentally from this equation:

$$\xi = \frac{E_2}{2\,E_1} \qquad (6)$$

The mechanical behavior of each layer is then modeled by a linear elastic law with Rayleigh damping in all layers, with damping coefficients determined at a frequency of 33 Hz, and the temperature 18 °C. Results give 19% for AC_1, 12% for the AC_2, 5% for the UGA and 3% for the subgrade.

4.2. Study of the damping effect

Results on the deflection basin are shown in Fig. 5. The damping affects the peak value of the pavement deflection, and the elastic wave propagation in the structure. However, the numerical results show that there is a minor influence on the phase, with very small delays of the load in G1: delays do not exceed 2 ms in the worst case, far from the load, on the geophone G9 (see Fig. 6 and 7).

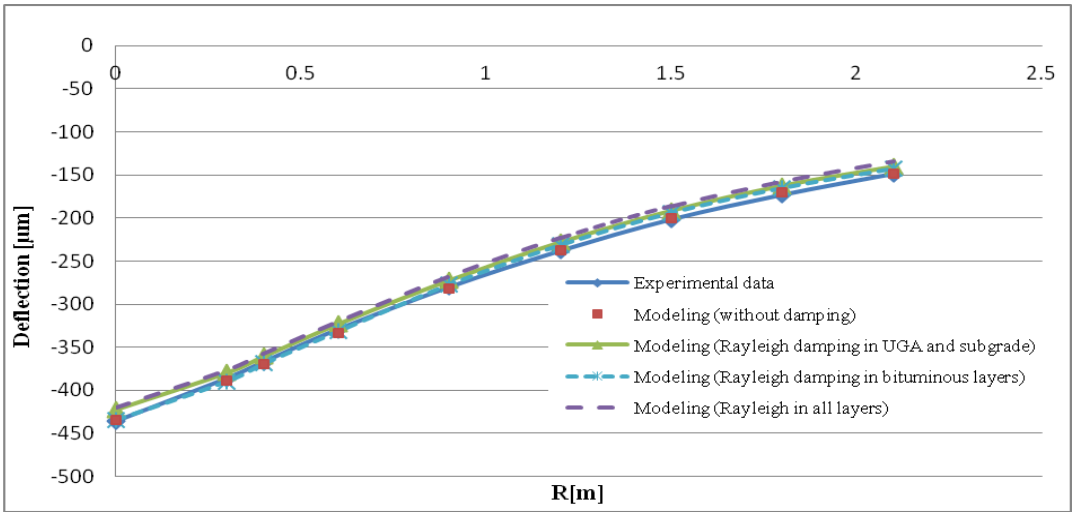

Fig. 5. Effect of the Rayleigh damping on the maximum deflection amplitude

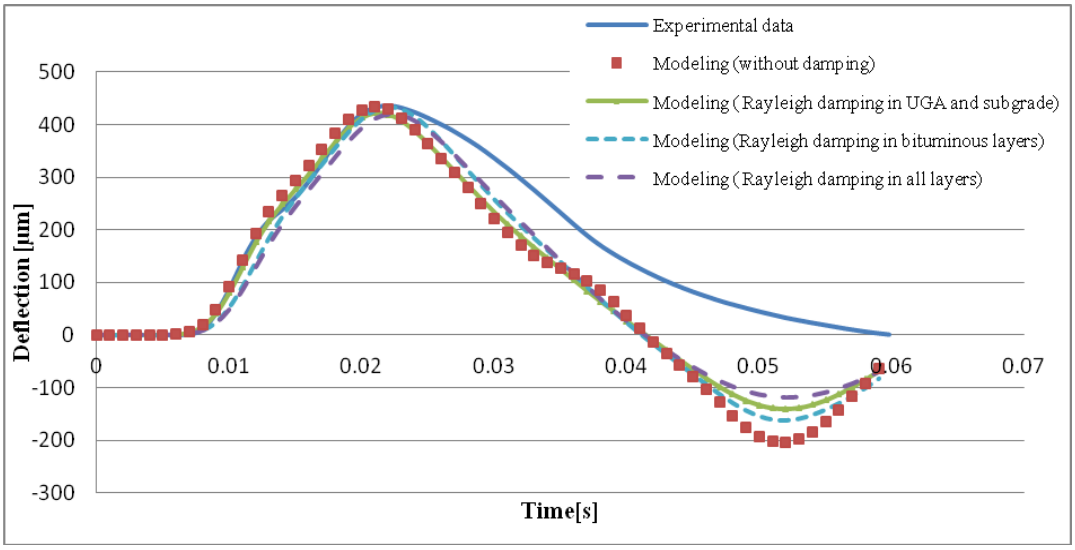

Fig. 6. Effect of Rayleigh damping on the history of deflections on central geophone G1

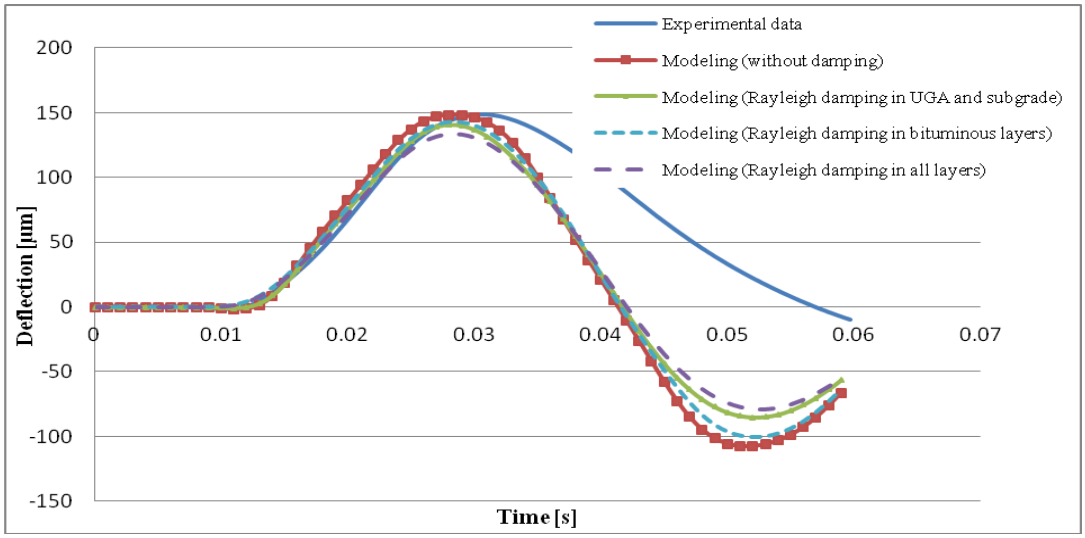

Fig. 7. Effect of Rayleigh damping on the history of deflections on farthest geophone G9

This preliminary study shows that the effect of Rayleigh damping affects the deflections magnitudes. The values of the damping coefficients were selected in the specific range: from 3 to 30% for the soil and 5 to 30% for the UGA although the upper values are unrealistic.
Fig. 8 shows that the increase in the value of the damping coefficient induces strong decreases in deflection amplitudes. This decrease is more important far from the loading area. For example, at R = 2.1 m, decrease is more than 17% for ξ = 3% (soil) and 5% (UGA) against 65% for ξ = 30% for both layers. It is only 13% and 48% at R = 0 m in the same conditions. Deflections are inversely proportional to the damping values. These results are in accordance with the sensitivity analysis of the model PAVDYN2D.

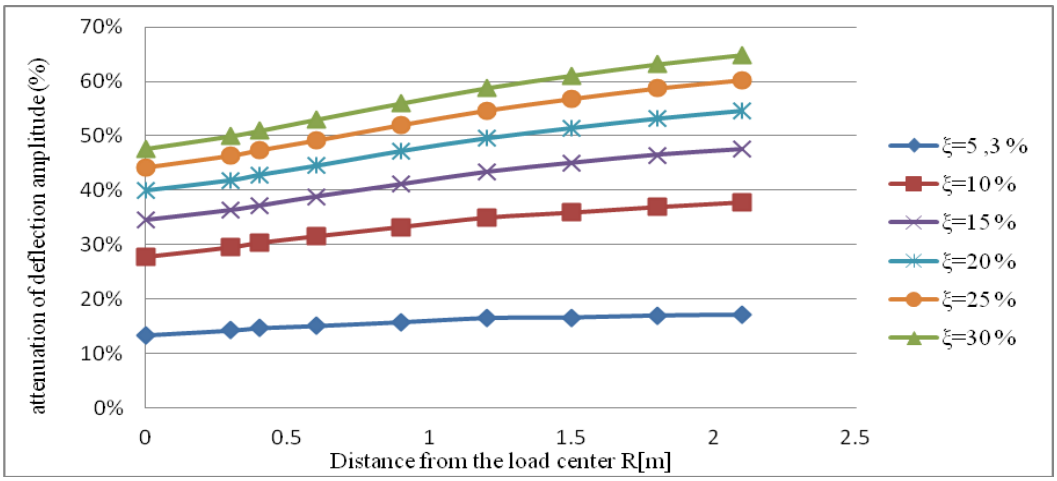

Fig. 8. attenuation of deflections amplitude against the distance to the load center for different damping coefficient ξ from 3 to 30 % for granular materials (UGA and Subgrade)

5. Viscoelastic damping

5.1. Presentation of the rheological model

The laboratory study of the behavior of asphalt under low amplitude sinusoidal stress carried out at various frequencies and temperatures, highlights the viscoelastic nature of these materials. Huet proposes in Huet (1963) to describe the shape of the complex moduli curvein the Cole & Cole chart, with a four parameter equation:

$$E^*(w) = \frac{E_\infty}{1+\delta(i\omega a(T))^{-k}+(i\omega a(T))^{-h}} \qquad (7)$$

Where:

- $E^*(w)$ is the complex modulus,
- E_∞ : parameter representing the complex modulus value when $\omega a(T) \to +\infty$,
- h, k : positive exponents lower than 1, related to the factor $\frac{\pi}{2}$ near the tangent at E=0 and E = E_∞ of complex modulus curve with the x-axis, and h>k,
- δ : real parameter model,
- $a(T)$: the construction of the master curve is effected through simple parallel translation to the frequency axis of a logarithmic chart in which the amplitudes depend on the temperature at experimental point. These back translations multiplying each frequency by a factor $a(T)$, called shift factor. The identification of the parameters does not require at this step to know the function.

Note that, by construction, these curves tend towards the origin as ω tends towards 0. The fitting is not very accurate at low frequencies, since the asphalt has a static modulus which is not taken into account in the Huet formula.

The Huet model is improved in Sayegh (1965) by adding a spring element in parallel, with very low stiffness compared to E_∞, to take into account this behavior for low frequencies.
The complex modulus is expressed as:

$$E^*(w) = E_0 + \frac{E_\infty - E_0}{1+\delta(i\omega a(T))^{-k}+(i\omega a(T))^{-h}} \quad (8)$$

Where E_0 is the complex modulus value when $\omega a(T) \to 0$.
The last model named Huet-Sayegh, allows better calibration with the experimental results but requires the adjustment of a fifth parameter. It is here suggested to use a simplified model of Huet & Sayegh. The complex modulus is expressed in equation (9) as a function of three parameters which are determined by calibration with the master curve (equation 11 and 12) of the asphalt concrete studied, such as:

$$E^*(w) = \frac{E_\infty}{1+A(iw)^{-\alpha}} = E_1 + i\,E_2 \quad (9)$$

with $$E_1 = \frac{E_\infty(1+Aw^{-\alpha}\cos(\alpha\frac{\pi}{2}))}{1+2Aw^{-\alpha}\cos(\alpha\frac{\pi}{2})+(Aw^{-\alpha})^2}, \quad E_2 = \frac{-i\,E_\infty Aw^{-\alpha}.\sin(\alpha\frac{\pi}{2})}{1+2Aw^{-\alpha}\cos(\alpha\frac{\pi}{2})+(Aw^{-\alpha})^2} \quad (10)$$

$$|E^*(w)| = \frac{E_\infty}{\sqrt{1+2Aw^{-\alpha}\cos(\alpha\frac{\pi}{2})+(Aw^{-\alpha})^2}} \quad (11)$$

$$\tan(\Phi) = \frac{-i\,Aw^{-\alpha}.\sin(\alpha\frac{\pi}{2})}{(1+Aw^{-\alpha}\cos(\alpha\frac{\pi}{2}))} \quad (12)$$

5.2. Adjustment parameters of viscoelastic model

Viscoelastic model parameters of simplified Huet-Sayegh are adjusted for bituminous concrete using the results of tests carried out by the LCPC from the STAC's instrumented facility (Broutin (2010)). The values of these parameters are presented in Table 2.

Table 2: simplified Huet-Sayegh parameters of the surface asphalt concrete (AC1 and AC2) at T=15°C

	E_∞	A	α
AC_1	**30378,889**	**8,623**	**0,343**
AC_2	**31859,653**	**4,733**	**0,339**

Figures 9 and 10 show the correspondence between the couples (| E *|, frequency) and (| E *|, phase) calculated with the rheological model and those measured in the laboratory for bituminous concrete.

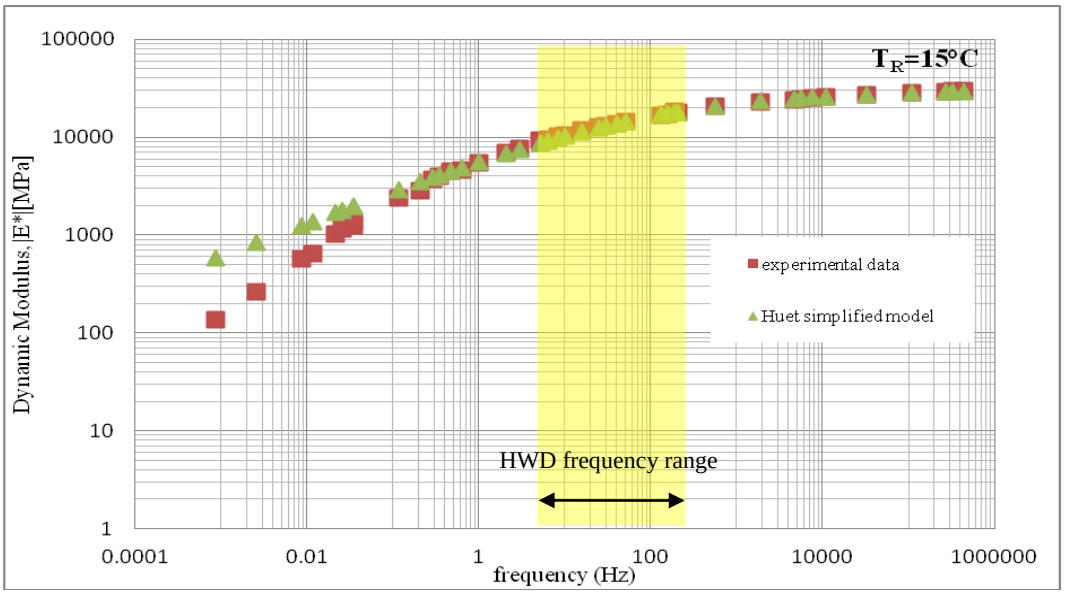

Fig. 9. Master curve (|E*|) of asphalt concrete (AC1) with the simplified Huet-Sayegh model at T=15°C.

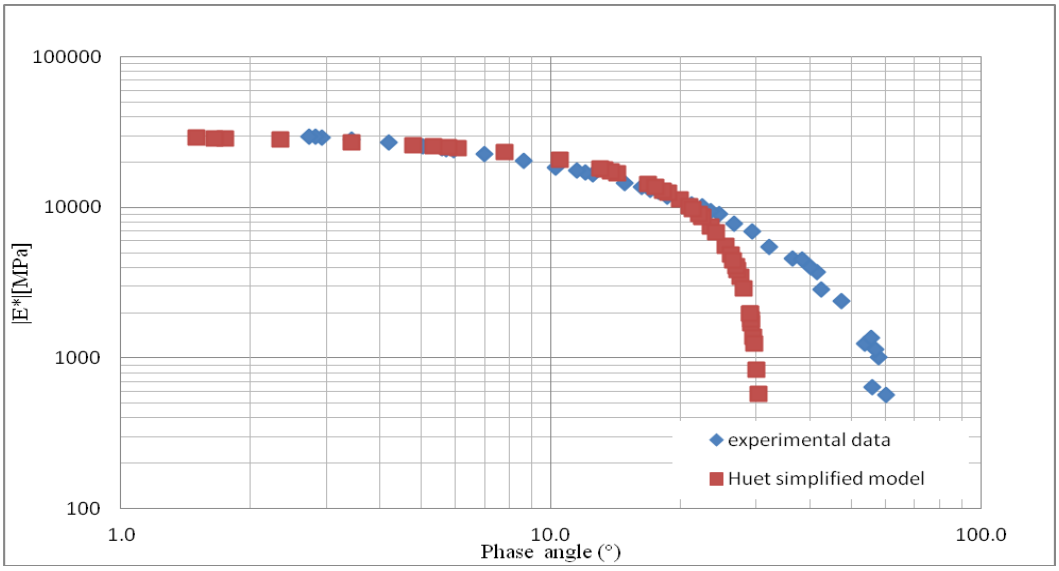

Fig. 10. Dynamic modulus and phase angle of asphalt concrete (AC1) in the Black domain

5.3. Methodology resolution in the frequency domain

The HWD pressure history signal is transformed into the frequency domain using the Fast Fourier Transform FFT, such as:

$$F(t) = F_0\, e^{i\omega t} \Rightarrow \tilde{F}(\omega) = \tilde{F}_r(\omega) + i\,\tilde{F}_i(\omega) \qquad (13)$$

The dynamic equation may be written as a system, with unknown real coefficients (constant damping):

$$\begin{bmatrix} K-\omega^2 M & \omega C \\ -\omega C & K-\omega^2 M \end{bmatrix} \begin{Bmatrix} \tilde{U}_r \\ \tilde{U}_i \end{Bmatrix} = \begin{Bmatrix} \tilde{F}_r \\ \tilde{F}_i \end{Bmatrix} \qquad (14)$$

The resolution of the system (14) is then carried out by an iterative process by solving the real part and the imaginary part separately. The stiffness matrices of the surface layers are frequency dependent due to the consideration of complex moduli given by the simplified Huet-Sayegh model (Equation 11). In the end, the required solution of the form $\tilde{U}_r(\omega) + i\,\tilde{U}_i(\omega)$ is reconstructed in the physical time domain by Inverse Fourier Transform.

5.4. Analysis of results

Each bituminous material is modeled using the viscoelastic simplified Huet & Sayegh model (frequency dependent). Soil and untreated materials layers are modeled with Rayleigh damping (5% for UGA and 3% for the Subgrade). Absorbing boundaries at the edges of the field are modeled to avoid reflections. Figure 11 shows a comparison between the "direct calculation" (frequency-domain resolution) of deflection basins with and without taking into account the viscoelasticity, in comparison with previous results without damping (time-domain resolution) and the experimental data. The results show that the viscoelasticity of bituminous materials induces a decrease in the amplitude of the deflections near the load center. Thus, a high attenuation is recorded in the vicinity of the load (over 25% in the center of the load and 20% to 0.4 m). These attenuations decrease far from the load center, reaching about 2.4% to 1.8 m.

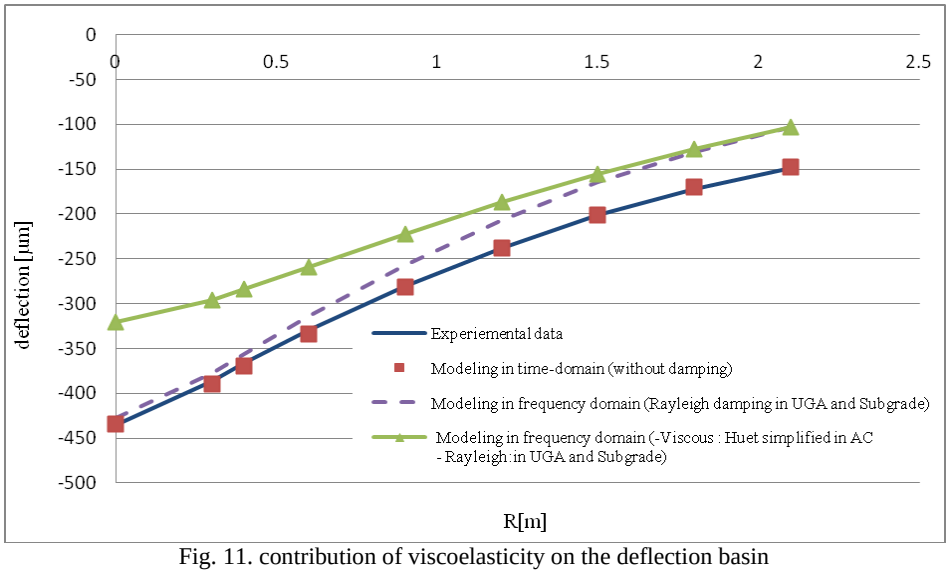

Fig. 11. contribution of viscoelasticity on the deflection basin

Fig. 12 also shows that the attenuation of the amplitude of deflection is linearly dependent on the distance from the load center.

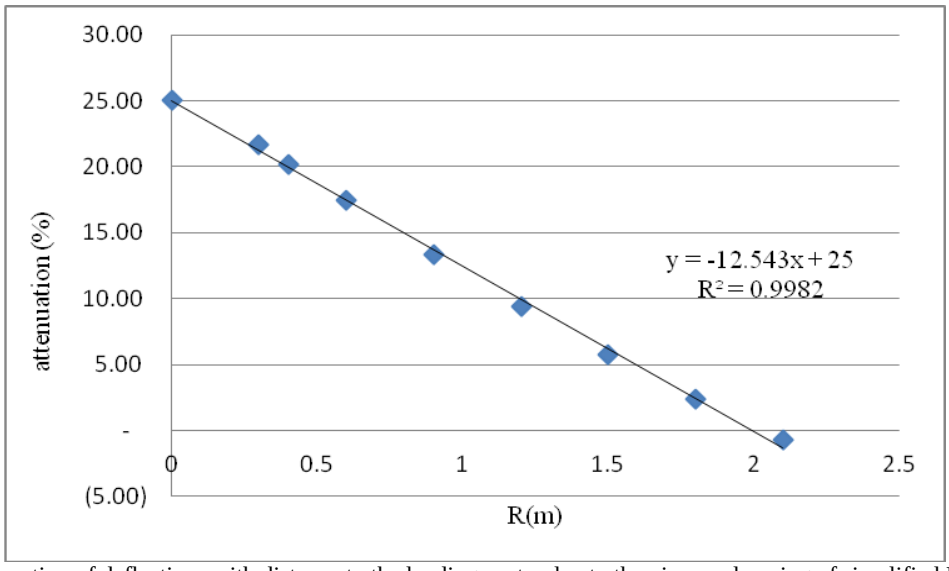

Fig. 12. attenuation of deflections with distance to the loading center due to the viscous damping of simplified Huet model.

6. Conclusion

This study implements a more realistic dynamic modeling of behavior of a multilayered pavement structure. Two types of damping were introduced: Rayleigh damping for layers of untreated material (subgrade and UGA) and viscoelastic damping based on the simplified Huet model for bituminous materials layers (asphalt concrete AC). The effect of Rayleigh damping is demonstrated in basins and deflection histories for different geophones. Introduction of the bituminous materials viscoelasticity showed a decrease in the deflection amplitude measured by the geophones located near the load area. This attenuation is linear as a function of the distance to the load center. The benefits of viscoelastic damping on the deflection history by taking into account the Huet-Sayegh model strongly depends on the considered frequency. This may lead to further developments using a modal basis resolution. The purpose will be to determine the viscoelastic mechanical properties (master curve) of asphalt materials directly from HWD device, thanks to a double criteria backcalculation (deflection basin and history signal).

References

Broutin M. Caron C. and Deffieux J.C. (2008). Dynamic versus static testing of airfield pavements: a full-scale experiment in France, *European Road Review*, fall 2008; 13: 17-25.

Broutin M. (2010). Assessment of flexible airfield pavement using Heavy Weight Deflectometers. Ph.D. Thesis, ENPC.

Chatti K. Mahoney JP. Monismith CL. Moran T. (1995) Field response and dynamic modeling of an asphalt concrete pavement section under moving heavy trucks, Proc of the International Symposium on Heavy Vehicle Weights and Dimensions ; 189-200.

Chen EYG. Pan E. Norfolk TS. Wang Q. (2011). Surface loading of a multilayered viscoelastic pavement moving dynamic load, Road Materials and Pavement Design ; 12(4): 849-874.

Chupin O. Chabot A. Piau JM. Duhamel D. (2010). Influence of sliding interfaces on the response of a layered viscoelastic meduim under a moving load, International Journal of solids and structures; 47(25-26), 3435-3446.

Combescure D. (2006). Eléments de dynamique des structures Illustrations à l'aide de Cast3M; http://www-cast3m.cea.fr/html/Combescure/DynamiqueCAST3MSeptembre2006.pdf. [in French].

Duhamel D. Chabot A. Tamagny P. Harfouche L. (2005) Viscoroute: Modélisation des chaussées bitumineuses, Bulletin de liaison des Ponts et chausses 2005 ; 89-103.

El-Ayadi A. (2010). Apport de l'analyse dynamique pour le diagnostic des chaussées. Ph.D. Thesis, Université de Limoges [in French].

Humbert P. Fezans G. Dubouchet A. et Remaud D. CESAR-LCPC. A computation software package dedicated to civil engineering uses. Bulletin of LCPC 2005; 256-257: 7-37.

Grenier S. Konrad J. LeBœuf D. Dynamic simulation of falling weight deflectometer tests on flexible pavements using the spectral element method: Forward calculations, Canadian Journal of Civil Engineering 2009; 36(6): 944-956.

Huet C. (1963). Etude par une méthode d'impédance du comportement viscoélastique des matériaux hydrocarbonés. Ph.D. Thesis, Faculté des sciences de l'université de Paris [in French].

Sayegh G. (1965). Contribution à l'étude des propriétés viscoélastiques des bitumes purs et des bétons bitumineux, Ph.D. Thesis, Faculté des sciences de l'université de Paris [in French].